Glassy behavior of the site frustrated percolation model

Silvia Scarpetta,[1,2,3] Antonio de Candia,[3,4] and Antonio Coniglio[3,4]
[1]*Dipartimento di Fisica Teorica, via S. Allende, 84081 Baronissi (SA), Italy*
[2]*INFM, Sezione di Salerno, Salerno, Italy*
[3]*Dipartimento di Fisica, Mostra d'Oltremare pad. 19, 80125 Napoli, Italy*
[4]*INFM, Sezione di Napoli, Napoli, Italy*
(Received 6 November 1996)

The dynamical properties of the site frustrated percolation model are investigated and compared with those of glass-forming liquids. When the density of the particles on the lattice becomes high enough, the dynamics of the model becomes very slow, due to geometrical constraints, and rearrangement on large scales is needed to allow relaxation. The autocorrelation functions, the specific volume for different cooling rates, and the mean-square displacement are evaluated and are found to exhibit glassy behavior. [S1063-651X(97)10803-0]

PACS number(s): 05.50.+q, 61.20.Ja, 64.70.Pf, 64.60.Ak

I. INTRODUCTION

Frustration plays a central role in many complex systems, such as spin glasses [1] and glass-forming liquids [2]. In spin glasses frustration arises because ferromagnetic and antiferromagnetic interactions are distributed in such a way that the spins cannot simultaneously satisfy all interactions. In glass-forming liquids frustration arises when local arrangements of molecules kinetically prevent all the molecules from reaching ordered close-packed configurations.

In this paper we study a lattice-gas model that contains frustration as an essential ingredient. This model is the site version of the bond frustrated percolation model, which was defined in the context of the generalization of the Fortuin-Kasteleyn [3] Coniglio-Klein [4] cluster formulation to the spin-glass model [5].

More precisely, consider the Ising spin-glass Hamiltonian

$$H=-J\sum_{\langle ij\rangle}\epsilon_{ij}S_iS_j, \tag{1}$$

where ϵ_{ij} are quenched random interactions that assume the values ± 1 with equal probability. By introducing bond variables between each nearest-neighbor pair of spins, it is possible to show that the spin-glass partition function can be expressed as a sum over bond configurations on the lattice [5]

$$Z=\sum_{C}{}^{*}e^{\beta\mu n(C)}q^{N(C)}, \tag{2}$$

where $q=2$ is the multiplicity of the spins, $\beta\mu=\ln(e^{q\beta J}-1)$, and $n(C)$ and $N(C)$ are, respectively, the number of bonds and the number of clusters in the bond configuration C. The asterisk in Eq. (2) means that the sum extends over all the bond configurations that do not contain a ''frustrated loop.'' This is defined as a closed path of bonds that contains an odd number of antiferromagnetic interactions. In this formalism the spin-glass problem is mapped onto a particular bond percolation problem, where each configuration of bonds has a weight $W(C)=e^{\beta\mu n(C)}q^{N(C)}$ if the configuration of bonds C does not contain a frustrated loop; otherwise $W(C)=0$.

For general values of q the model has been called ''q-bond frustrated percolation'' [6] and the partition function (2) can be obtained from a Hamiltonian model in which, besides the Ising spins interacting in a spin-glass way, there are Potts spins in each site, interacting ferromagnetically, with multiplicity $s=q/2$ [7].

The model exhibits two critical points for each value of q: one at higher temperature $T_p(q)$, corresponding to the percolation transition, in the same universality class as the ferromagnetic Potts model with multiplicity $s=q/2$, and one at lower temperature $T_{\mathrm{SG}}(q)$, in the same universality class as the Ising spin-glass transition. This has been verified by renormalization methods [8] and numerically [9].

It has also been shown [7,8] that for $q\neq 2$ the percolation transition corresponds to a singularity in the partition function and thus corresponds to a real thermodynamic transition. Each critical point is characterized by a diverging length, associated with the quantities [7,6]

$$p_{ij}=p_{ij}^{+}+p_{ij}^{-} \tag{3}$$

and

$$g_{ij}=p_{ij}^{+}-p_{ij}^{-}. \tag{4}$$

Here p_{ij}^{+} (p_{ij}^{-}) is the probability that (i) sites i and j are connected by at least one path of bonds and (ii) the phase η_{ij} defined as the product over all the signs ϵ_{mn} along the path connecting i and j is $+1$ (-1) [10].

The length ξ_p associated with the pair connectedness function $\overline{p_{ij}}$ diverges at the percolation critical point, while the length ξ associated with $\overline{g_{ij}^2}$ diverges at $T_{\mathrm{SG}}(q)$ (the overbar represents the average over all possible interaction configurations $\{\epsilon_{ij}\}$). For $q=2$ the quantity g_{ij} in Eq. (4) coincides with the spin-spin pair-correlation function.

However, we can give a geometrical interpretation of the second length ξ. The second transition, like the quantum percolation transition [11], occurs at a bond density higher than the usual percolation transition, due to the interference

of paths with different phases. At high density the number of allowed configurations is extremely reduced and most of the configurations connecting a given pair of sites i and j will have a common path. We call this path a ''quasifrozen'' path, since in a dynamical sequence of configurations exploring the allowed phase space, this path will be present most of the time. In conclusion, the major contribution to g_{ij} is due to those configurations in which i and j are connected by quasifrozen bonds [6,12,13] and $|\overline{g_{ij}}|$ roughly coincides with the probability that i and j belong to the same quasifrozen cluster, and the length ξ associated with $\overline{g_{ij}^2}$ roughly represents the linear dimension of these clusters. For $q=1$ Eq. (2) reduces to the bond frustrated percolation model, in which bonds are randomly distributed on the lattice, with the only constraint that configurations of bonds that contains at least one frustrated loop are not allowed [14].

Thus the model incorporates in the simplest way the concepts of geometrical frustration and could be applied to those systems, such as glass-forming liquids, where geometrical frustration due to packing problems plays a central role. We note that in this model the disorder is quenched, while in glass-forming liquids this is not the case. However, at low temperature or high density the relaxation times are so large that the disorder may be considered frozen in.

To better describe the particle nature of glassy systems, we have introduced in this paper the site version of the frustrated percolation model, in which sites can be full or empty. Full sites can be seen as ''particles'' and empty sites as vacancies. We leave unchanged the underlying structure of the interactions and the constraint that no frustrated loop can be fully occupied. We consider in this paper only the $q=1$ case.

In Sec. II we introduce the model and in Sec. III we describe two types of Monte Carlo dynamics (thermalization and diffusion dynamics) used to simulate the model. We study the static properties of the system in Sec. IV. In particular, we verify that the percolation transition is in the same universality class as the $s=1/2$ ferromagnetic Potts model. The cooling rate dependence of the specific volume is considered in Sec. V, while in Sec. VI we analyze the diffusion dynamics of the model, evaluating the mean-square displacement of the particles and the diffusion coefficient. Finally, in Sec. VII we evaluate the autocorrelation functions of density fluctuations, in both thermalization and diffusion dynamics, which show a behavior typical of glass-forming liquids. In the Appendix we describe in more detail the Monte Carlo procedure.

II. THE SITE FRUSTRATED PERCOLATION MODEL

In the site frustrated percolation (SFP) model particles are introduced on the vertices of a regular lattice. We assign to each edge of the lattice an interaction $\epsilon_{ij}=\pm 1$, positive or negative according to a random quenched distribution. Like in spin glasses a frustrated loop is a closed path of edges that contains an odd number of negative interactions. A particle configuration is forbidden only if it contains a fully occupied frustrated loop [15] (see Fig. 1). Thus we assign zero weight to all configurations of particles that contain at least one fully occupied frustrated loop and to all other configurations a weight

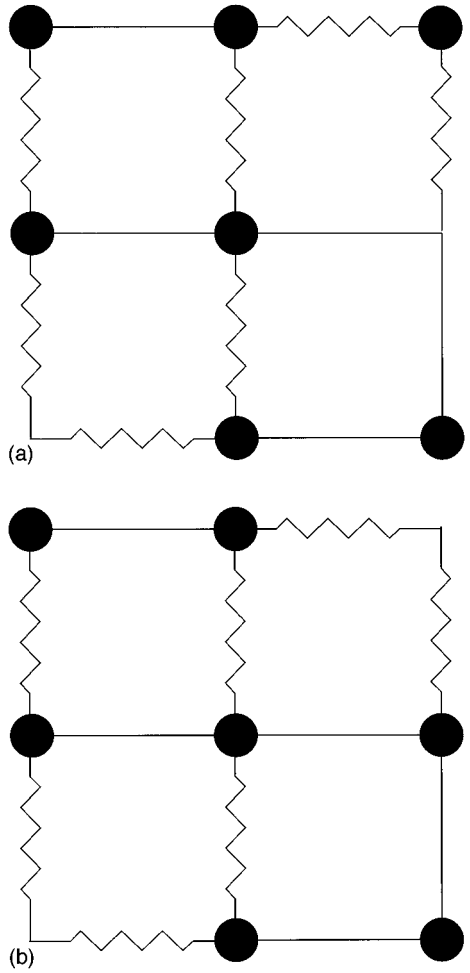

FIG. 1. (a) Site configuration that does not contain frustrated loops (permitted) and (b) site configuration that contains a frustrated loop (forbidden).

$$W(C)=e^{\beta\mu n(C)}, \tag{5}$$

where $n(C)$ is the number of particles in the configuration C, μ is the chemical potential of the particles, and $\beta=1/k_BT$. The partition function of the model is given by

$$Z=\sum_C {}^*e^{\beta\mu n(C)}, \tag{6}$$

where the sum excludes forbidden configurations.

Note that there is only one independent parameter $\beta\mu$, which can vary from $-\infty$ to ∞. Frustration prevents the system from reaching a maximum density $\rho=1$ for $\beta\mu\to\infty$: when $\beta\mu$ varies from $-\infty$ to ∞, the density $\rho=\langle n\rangle$ varies from 0 to $\rho_{\max}<1$.

The SFP model is expected to have two critical points, in analogy to the bond case [7–9]. Fixing the value of μ to a positive value and varying the temperature from high to low values, there is a first critical point at a temperature T_p, corresponding to the percolation transition, and one at lower temperature $T_{\rm SG}$, corresponding to a spin-glass transition. The percolation transition is expected to be in the same universality class as the ferromagnetic $s=1/2$ ferromagnetic Potts model, while in two dimensions $T_{\rm SG}$ is expected to

occur at $T=0$. At low temperature the model is expected to have the characteristic features of a spin-glass system, such as a rough free-energy landscape, very long relaxation times due to the high-free-energy barriers, and many ground states at $T=0$.

III. MONTE CARLO DYNAMICS

We have realized two types of Monte Carlo dynamics to simulate the SFP model. The first, which we call ''thermalization dynamics,'' proceeds through the following steps. (i) Pick up a site at random. (ii) If the site is filled by a particle, destroy that particle with probability P_- or leave the site filled with probability $(1-P_-)$. (iii) If the site is empty, leave it empty if a new particle placed in that site would close a frustrated loop; otherwise, if the particle would not close a frustrated loop, create a new particle in that site with probability P_+ or leave the site empty with probability $(1-P_+)$. Looking at the partition function (6), it is easy to verify that the following probabilities of creating or destroying a particle satisfy the principle of detailed balance:

$$P_-=1, \quad P_+=e^{\beta\mu} \quad \text{for} \quad \beta\mu<0, \tag{7a}$$

$$P_-=e^{-\beta\mu}, \quad P_+=1 \quad \text{for} \quad \beta\mu>0. \tag{7b}$$

This dynamics is clearly ergodic because we can go from a permitted configuration A to a permitted configuration B, first destroying the particles belonging to A and then creating those belonging to B.

The difficult step here is to verify that a new particle does not close a frustrated loop since this involves a nonlocal check. The procedure is described in the Appendix.

The second type of Monte Carlo dynamics, which we call ''diffusion dynamics,'' starts from a site configuration with some density ρ of particles, obtained by thermalization dynamics, and proceeds by letting the particles diffuse conserving their number. At each step a site is chosen at random; if the site is filled, we make an attempt to move the particle to a nearest-neighbor (NN) site. The move is accepted if the probed site is empty and no frustrated loop is closed.

IV. PERCOLATION TRANSITION AND EQUILIBRIUM DENSITY

In this section we analyze the percolation properties of the model. The analysis of the data confirms that the percolation transition, for the site frustrated percolation problem, is in the same universality class as the ferromagnetic $s=1/2$ Potts model, as was formerly verified for the bond problem [9].

We have used the histogram method for analyzing data [16]. For various lattice sizes, we simulated the system using thermalization dynamics for ten temperatures around the percolation point. For each temperature we reached equilibrium by taking 10^4 steps and then evaluated the histograms of the following quantities, taking 10^5 steps: density of particles ρ, probability of existence of a spanning cluster P_∞, and mean cluster size χ. The mean cluster size is defined as

$$\chi=\frac{1}{N}\sum_s s^2 n_s, \tag{8}$$

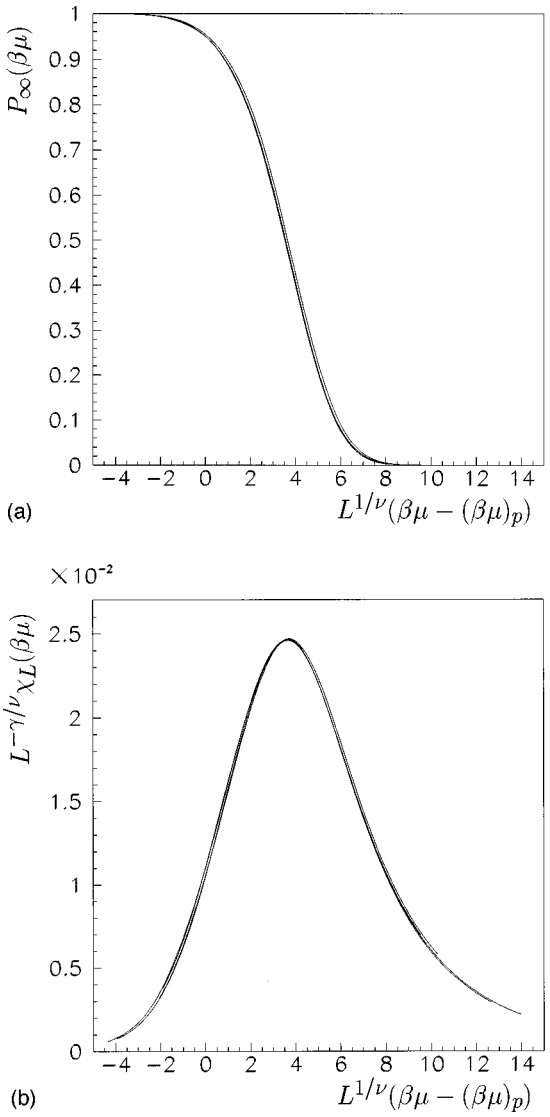

FIG. 2. (a) Finite-size scaling of the probability that a spanning cluster exists and (b) finite-size scaling of the mean cluster size.

where n_s is the number of clusters having size s in the system.

Using the histogram method [16], we evaluated the values of these three quantities for an entire interval of the parameter $\beta\mu$. Shown in Fig. 2 is the finite-size scaling of P_∞ and of χ, from which it is possible to extract the values of the critical temperature, and of the critical exponents ν and γ [17].

The data are perfectly compatible with the values $\nu^{-1}=0.56$ and $\gamma=3.27$ of the $s=1/2$ Potts model [18]. The critical (percolation) value for $\beta\mu$ is found to be $(\beta\mu)_p=1.2$, which corresponds to a density $\rho_p\simeq 0.6$, which is, within the error, not different from the percolation density of the standard random site percolation $\rho_p=0.593$ [19].

We evaluated the equilibrium density of the SFP, varying the parameter $\beta\mu$ from $\beta\mu=-15$ to $\beta\mu=15$, with a rate 3×10^{-5} step^{-1}. The result is shown in Fig. 3. For comparison we plot also the equilibrium density of the unfrustrated model, which is given by $\rho=1/(1+e^{-\beta\mu})$. This curve fits quite well the low-density part, since for low density the effect of frustration is negligible. The high-density part in-

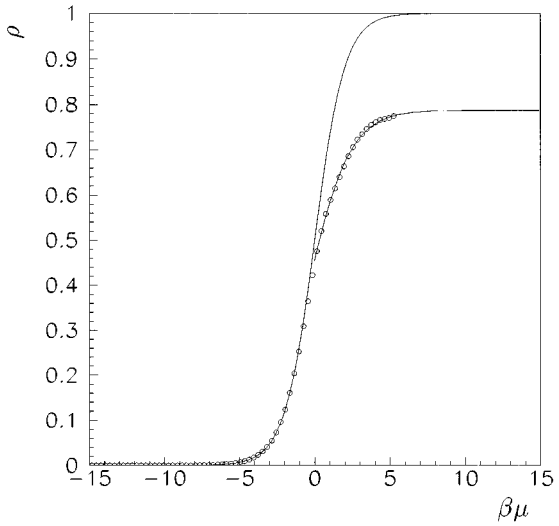

FIG. 3. Equilibrium density of the SFP as a function of $\beta\mu$ (circles), together with the fit function (lower curve). The upper curve is the density of the unfrustrated model.

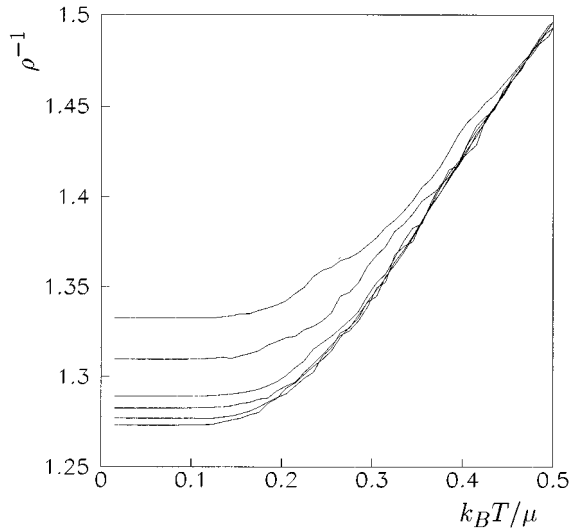

FIG. 4. Temperature dependence of the specific volume ρ^{-1} in the SFP model (32×32 square lattice), for various cooling rates. From upper curves to lower ones: $k_B\dot{T}/\mu=10^{-2}$, 10^{-3}, 10^{-4}, 10^{-5}, 10^{-6}, and 10^{-7} step^{-1}.

stead is better fitted by the function

$$\rho=\frac{\rho_{\max}}{1+e^{-a-b(\beta\mu)}}, \tag{9}$$

where $\rho_{\max}=0.788$, $a=0.323$, and $b=0.719$. Note from Fig. 3 that the crossover occurs at a value of $\beta\mu$, close to the percolation threshold.

V. COOLING RATE DEPENDENCE OF THE DENSITY

The effect of frustration prevents the system from *easily* reaching the equilibrium density, especially at very high values of the parameter $\beta\mu$, that is, for $\beta\mu\to\infty$. Fixing μ to a positive value and cooling the temperature from high to low values with a finite cooling rate, there is a temperature T_G at which the system goes out of equilibrium. Lowering the temperature further, the density remains constant to the value corresponding to the temperature T_G.

Figure 4 shows the temperature dependence of the density for various cooling rates. Temperature goes from $k_BT/\mu=0.5$ to $k_BT/\mu=0$ and cooling rates range from $k_B\dot{T}/\mu=10^{-2}$ to 10^{-7} step^{-1}. One step is one update per site.

This behavior is experimentally observed in supercooled glass-forming liquids, at the calorimetric glass transition temperature T_G, when structural relaxation times become greater than the experimental observation times [20]. As in glass-forming liquids, in the model we observe that the faster the cooling rate, the greater the glass transition temperature and the specific volume.

VI. DIFFUSION DYNAMICS

We then studied the diffusion dynamics (conserved number of particles) of the system. The diffusion process is severely hindered by kinetic constraints at high density and particles can diffuse through the system only by a large-scale cooperative rearrangement of many particles. At low density we expect that the effect of frustration on the diffusion is very weak because of abundance of holes and particles diffuse freely on the lattice.

We have evaluated the mean-square displacement (MSD) $\langle\Delta r(t)^2\rangle$ as a function of time t, as shown in Fig. 5. Each curve is obtained averaging over all the particles and over a time interval of 5000 steps. As expected for low density, the curves show a linear behavior, which corresponds to normal diffusion. For high densities, the MSD reaches a plateau and then becomes again linearly dependent on time. This behavior is typical of glass-forming liquids and is also observed in molecular-dynamics simulations [21,22]. The crossover from the normal behavior to the anomalous diffusion in our model again occurs at a density value close to percolation.

We have extrapolated the diffusion coefficient values

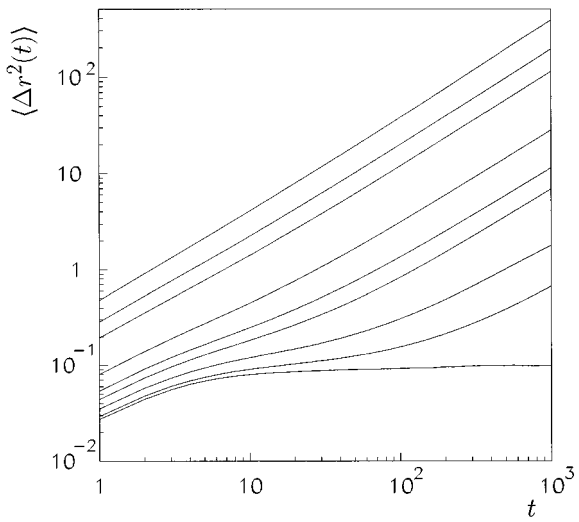

FIG. 5. Mean-square displacement $\langle\Delta r^2(t)\rangle$ as a function of time t, in the SFP model on a square lattice with $L=32$, for densities (from upper curves to lower ones) $\rho=0.452$, 0.586, 0.730, 0.756, 0.766, 0.777, 0.784, and 0.785.

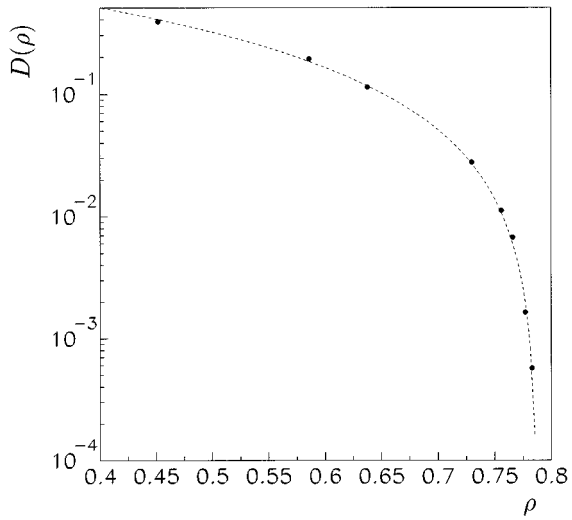

FIG. 6. Long-time diffusion coefficients D as a function of density ρ. The fit function is $D=2.14\times|\rho-0.7874|^{1.53}$.

$D=\langle\Delta r(t)^2\rangle/t$ from the long-time regime, which are shown in Fig. 6. The extrapolated values are very well fitted by a power law as a function of density

$$D\sim(\rho-\rho_c)^{\gamma}, \tag{10}$$

with $\rho_c\simeq 0.7874$ and $\gamma\simeq 1.5$.

Note that ρ_c is equal within the errors to $\rho_{\max}$, the density corresponding to the ground state, as extracted from the fit (9). Thus the dynamic singularity coincides in this model with the spin-glass transition, which in two dimensions occurs at $T=0$. If we set $\rho_c=\rho_{\max}$, using Eq. (9) we obtain from Eq. (10)

$$D\sim\left(1-\frac{1}{1+e^{-a-b(\beta\mu)}}\right)^{\gamma}\sim e^{-b\gamma(\beta\mu)}, \tag{11}$$

which shows that the diffusion coefficient goes to zero with an Arrhenius law for $T\rightarrow 0$.

The picture that emerges from the model is that particles are trapped most of the time in cages formed by their NN and can diffuse only into localized pockets. Only after a very long interval of time do they have the opportunity of escaping from the cage, falling in a ''next-neighbor'' cage. This process forms a kind of random walk, reflected in the long-time linear dependence of the MSD functions.

This picture is enforced by direct observation of the particles moving on the lattice. We have taken ''snapshots'' of the system at particular times, for diffusion dynamics at two high values of the density. Some particles leave tracks on the lattice, so we can analyze also the path they have taken. Shown in Fig. 7 is the snapshot at $\rho=0.783$ after 2000 steps [Fig. 7(a)], after 4000 steps [Fig. 7(b)] and at $\rho=0.785$ after 2000 steps [Fig. 7(c)].

We mark with dots the particles that moved at least one time (nonfrozen domains) during the time of the simulation; the filled circles represents frozen domains. Clusters of frozen particles prevent other particles from moving freely. We note that frozen particles are clustered and we can distinguish liquidlike zones (holes and mobile particles) from solidlike zones (frozen clusters). Frozen clusters are eroded as the time of the simulation gets longer, while liquidlike zones grow.

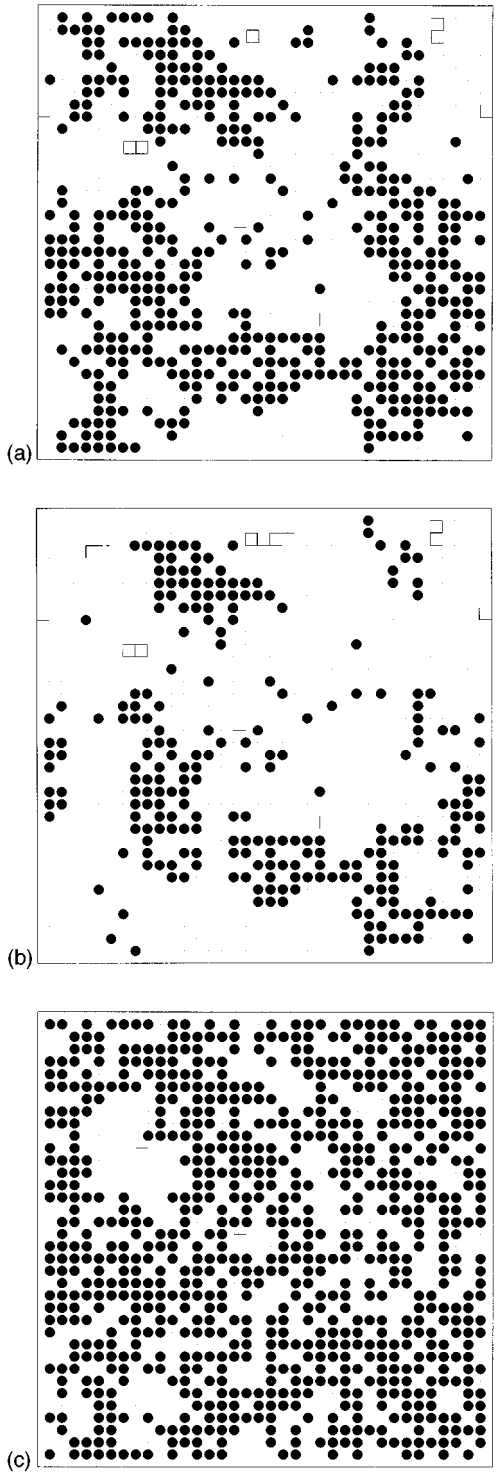

FIG. 7. Path of tagged particles at density $\rho=0.783$ after 2000 steps (a), after 4000 steps (b), and at $\rho=0.785$ after 2000 steps (c). Dots are particles that have moved at least one time in the time indicated (nonfrozen domains); the filled circles represent particles that have never moved in the time indicated (frozen domains) The frozen domains in (c) are still frozen after 2×10^5 steps.

At the very high density, frozen particles remain blocked for extremely long times. The frozen cluster in Fig. 7(c),

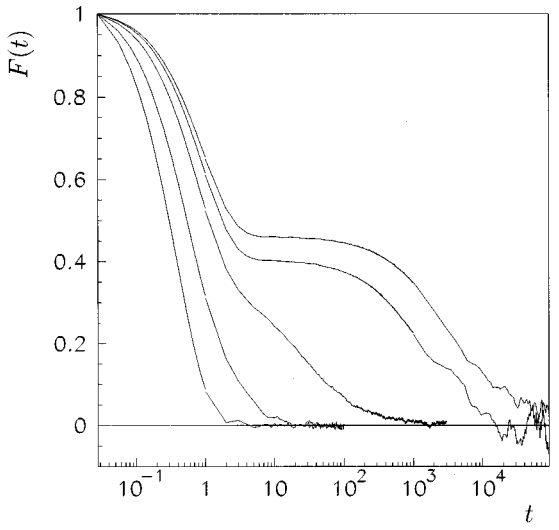

FIG. 8. Relaxation functions $F(t)$ of the site density as a function of time t, for the thermalization dynamics, on an $L=36$ square lattice, for temperatures between $e^{\beta\mu}=1$ and $e^{\beta\mu}=1000$, corresponding to equilibrium density (from lower to higher relaxation times): $\rho=0.450$, 0.639, 0.715, 0.782, and 0.784.

corresponding to density $\rho=0.785$, is still frozen after 2×10^5 steps, which corresponds to the maximum time we have observed. We have checked that the large frozen cluster does not percolate in either direction, even if the density of the frozen particles is much greater than the percolation density of the random site percolation. We expect that the frozen particles in fact percolate at $T=0$ ($\rho=\rho_{\max}$) since the linear dimension of the frozen cluster should correspond roughly to the correlation length associated with g_{ij} [Eq. (4)], which for $d=2$ is expected to diverge at $T_{\rm SG}=0$, as explained in the Introduction.

VII. RELAXATION FUNCTIONS

An important property that characterizes glassy behavior is the form of the relaxation functions [23–25]. We have evaluated the relaxation functions of the system, in the thermalization and in the diffusion dynamics. For each temperature, we reach the equilibrium and then evaluate the relaxation functions averaging on a time interval of 10^3-10^6 steps.

Figure 8 shows the density-density autocorrelation function in the thermalization dynamics, defined as

$$F(t)=\frac{\langle \delta\rho(t)\,\delta\rho(0)\rangle}{\langle \delta\rho^2\rangle}, \tag{12}$$

where $\delta\rho(t)=\rho(t)-\langle\rho\rangle$. For diffusion dynamics, we have studied the autocorrelation function of the density fluctuations

$$F_{\mathbf{k}}(t)=\frac{\langle \delta\rho_{\mathbf{k}}(t)\,\delta\rho_{-\mathbf{k}}(0)\rangle}{\langle \delta\rho_{\mathbf{k}}\delta\rho_{-\mathbf{k}}\rangle}, \tag{13}$$

where

$$\rho_{\mathbf{k}}(t)=\sum_{\alpha} e^{i\mathbf{k}\cdot\mathbf{r}_\alpha(t)} \tag{14}$$

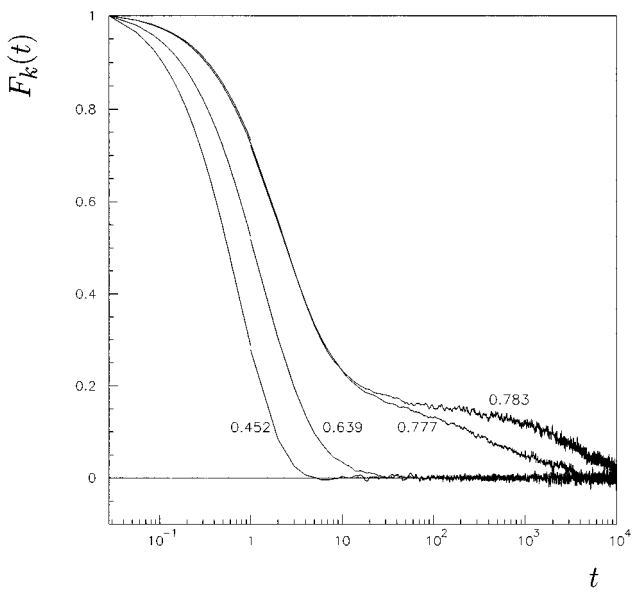

FIG. 9. Relaxation functions $F_{\mathbf{k}}(t)$ of the density fluctuations as a function of time t, for the diffusion dynamics, for densities $\rho=0.452$, 0.639, 0.777, and 0.784, on an $L=36$ square lattice and $k_x=\pi$, $k_y=0$.

and $\mathbf{r}_\alpha$ is the position of the αth particle in units of the lattice constant. The wave vector can take the values $\mathbf{k}=(2\pi/L)\mathbf{n}$, where $\mathbf{n}$ has integer components n_x and n_y ranging from 0 to $L/2$. The autocorrelation functions corresponding to $n_x=L/2$ and $n_y=0$ are reported in Fig. 9.

Figure 10 shows the self-part of the relaxation function in the diffusion dynamics, defined as

$$F^s_{\mathbf{k}}(t)=\frac{1}{n}\left\langle \sum_{\alpha} e^{i\mathbf{k}\cdot(\mathbf{r}_\alpha(t)-\mathbf{r}_\alpha(0))}\right\rangle, \tag{15}$$

where n is the number of particles. At low temperatures, below the percolation threshold, we observe the onset of

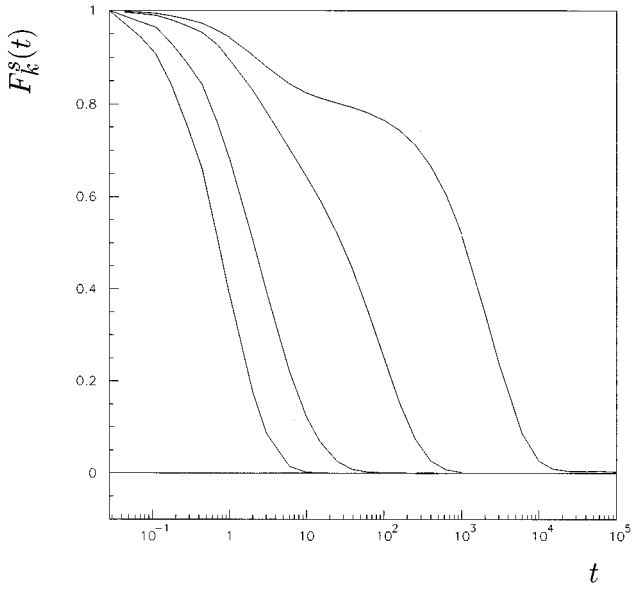

FIG. 10. Self-part $F^s_{\mathbf{k}}(t)$ of relaxation functions of the density fluctuations as a function of time, for the diffusion dynamics, for densities (from lower to higher relaxation times) $\rho=0.452$, 0.639, 0.757, and 0.783 on an $L=36$ square lattice, with $k_x=\pi$, $k_y=0$.

nonexponential decay. This is usually the sign of nonstochastic cooperative relaxation in the system. We emphasize that, for our model, the percolation transition corresponds to a real thermodynamic transition and therefore it is possible to expect, below this point, a change in the dynamical properties of the system.

Evident at very high density is the existence of different time regimes as predicted by the *mode-mode coupling* theory [26, 27] of supercooled liquids and observed both in some molecular-dynamic simulations and in some experimental measurement [23] on glass-forming liquids. There is a first short-time relaxation, corresponding to relaxation inside nonfrozen domains surrounded by a frozen cage, and a long-time regime (α relaxation), corresponding to structural rearrangement and final decay to equilibrium.

VIII. CONCLUSION

We have studied a frustrated lattice-gas model that has been called site frustrated percolation since percolation plays an important role. This model, despite its simplicity, shows a complex dynamical behavior. Disorder and frustration are its basic ingredients. The constraint of frustration prevents the system from easily reaching a high density and inhibits the motion of particles at a high density.

We observed that the dependence of the volume as a function of the temperature varies strongly with the cooling rate, qualitatively in the same way as observed in real glass-forming liquids. The motion of particles in diffusion dynamics is severely hindered by the frustration constraint and the relaxation process can take place only through large-scale rearrangement. The cooperative nature of the motion is reflected in the behavior of the mean-square displacement and in the relaxation functions of the system. The plateaus observed in the self-part of relaxation functions (Fig. 10) and in the mean-square displacement (Fig. 5) are intrinsically connected and are characteristic of the glassy nature of the dynamical properties of the model. In all these phenomena the crossover from a normal behavior to an anomalous behavior occurs close to or at the percolation threshold.

Since SFP seems to describe well the glass transition in glass-forming liquids, the model suggests that the presence of a percolation-type transition may be a general feature below which frustration effects start to be manifested. This transition may be responsible for various precursor phenomena [13], such as the onset of stretched exponentials, the breakdown of the Stokes-Einstein relation, and the presence of spatial heterogeneity.

The presence of a percolation transition well above the glass transition has recently been discovered by Tomida and Egami [28] in a molecular-dynamic simulation of monatomic liquids. It is also interesting to note that Kivelson *et al.* [29] showed that the viscosity of 15 glass-forming liquids could be collapsed on one single curve, by assuming only one characteristic temperature well above the glass transition. Finally, the ideal glass transition temperature, characterized by the divergence of the inverse of the diffusion coefficient, numerically seems consistent with the divergence of the static length ξ associated with g_{ij} [Eq. (4)].

Although we have discussed the site frustrated percolation model in the context of glassy systems, the model is rather generic and may be applied to other systems, where geometrical frustration plays an essential role. In fact, recently the model has been successfully applied also to granular materials [30].

ACKNOWLEDGMENTS

We would like to thank V. Cataudella, F. di Liberto, S. C. Glotzer, M. Nicodemi, and U. Pezzella for interesting discussions. This work has been supported in part by CNR.

APPENDIX

As mentioned in Sec. III, we describe here the procedure to check whether or not a new particle, added to the system in a given configuration, closes a frustrated loop.

Every NN particle (occupied site) of the empty site that has been probed to be filled, belongs to a (not necessarily distinct) cluster of connected sites. If two particles that are NN to the empty site belong to the same connected cluster, then a new particle filling that site closes a loop. More precisely, if z_n is the number of particle NN's to the empty site and z_c is the number of *distinct* clusters to which they belong, then the total number of new loops closed by the new particle is $\lambda = z_n - z_c$.

The algorithm proceeds as follows. We count the number z_n of particles that are NN to the empty site that we want to fill and mark each of them as the root of a distinct cluster, so at the beginning $z_c = z_n$ and $\lambda = 0$; we grow every cluster in parallel, adding to it in a recursive way its still not visited NN particles and marking them as belonging to that cluster; if no particle NN to a cluster is found, that cluster is marked as ''burnt'' and is not considered anymore; if two clusters collide, we say we have found a loop, the two clusters merge to form a single cluster, λ is increased by one and z_c is decreased by one. Every new visited site is marked in two ways: with the label of the cluster to which it belongs and with the ''parity,'' which is the number of antiferromagnetic interactions proceeded through starting from the initial empty site. We stop the iteration when one of the following circumstances happens: two clusters collide and the parities

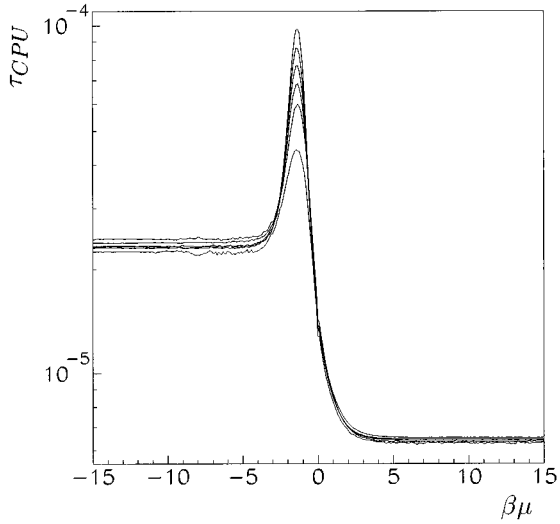

FIG. 11. CPU times needed to make a single-site update as a function of $\beta\mu$, for lattice sizes (from lower to upper curves) $L = 24,\ 32,\ 40,\ 48,\ 56$, and 64.

do not correspond (that is, one is odd and the other is even): in this case we have found a frustrated loop; the number of burnt clusters equals $z_c - 1$ (only one cluster is nonburnt): in this case no other loop can be found. When the density of particles is low, this algorithm is very fast since the clusters are very small and are burnt within few iterations. On the other hand, when the density is high, the maximum number of independent loop is found quickly as well. The algorithm can become slow when the density of particles is intermediate, notably near the percolation transition, because clusters in this case are very ramified. In Fig. 11 the CPU time needed to do a single-site update is shown for a square bidimensional system and for various lattice dimensions. The maximum time is reached near the percolation transition and scales as

$$\tau_{\max} \propto N^{0.40 \pm 0.05}, \tag{A1}$$

where $N = L^2$ is the total number of sites.

[1] K. Binder and A.P. Young, Rev. Mod. Phys. **58**, 801 (1986); M. Mezard, G. Parisi, and M.A. Virasoro, *Spin Glass Theory and Beyond* (World Scientific, Singapore, 1987).

[2] For a review see, for example, M.D. Ediger, C.A. Angell, and S.R. Nagel, J. Phys. Chem. **100**, 13 200 (1996).

[3] C.M. Fortuin and P.W. Kasteleyn, Physica **57**, 536 (1972).

[4] A. Coniglio and W. Klein, J. Phys. A **12**, 2775 (1980).

[5] A. Coniglio, F. di Liberto, G. Monroy, and F. Peruggi, Phys. Rev. B **44**, 12 605 (1991).

[6] A. Coniglio, *Nuovo Cimento* D **16**, 1027 (1994).

[7] V. Cataudella, A. Coniglio, L. de Arcangelis, and F. di Liberto, Physica A **192**, 167 (1993).

[8] A. Coniglio and U. Pezzella, Physica A (to be published).

[9] A. de Candia, doctoral thesis, University of Naples, 1994 (unpublished).

[10] If in a given configuration of bonds there is more than one path of bonds connecting i and j, it is straightforward to show that the resulting phase η_{ij} is path independent since the configuration does not contain frustrated loops.

[11] Y. Meir, A. Aharony, and A.B. Harris, Europhys. Lett. **10**, 275 (1989), and references therein.

[12] N. Jan, S.C. Glotzer, P.H. Poole, and A. Coniglio, Fractals **3**, 465 (1995).

[13] S.G. Glotzer and A. Coniglio, J. Comput. Mater. Sci. **4**, 324 (1995).

[14] In this case the percolation transition is in the same universality class as the ferromagnetic 1/2-state Potts model. A connection between the dilute spin glass at zero temperature and the 1/2-state Potts model has been discussed by A. Aharony and P. Pfeuty, J. Phys. C **12**, L125 (1979).

[15] It can be shown that this constraint can be induced by the ϵ_{ij} when these variables represent interactions between the particle's internal degree of freedom. See M. Nicodemi and A. Coniglio (unpublished).

[16] R.H. Swendsen, Physica A **194**, 53 (1993).

[17] K. Binder and D.W. Heermann, *Monte Carlo Simulations in Statistical Physics* (Springer-Verlag, Berlin, 1988).

[18] F.Y. Wu, Rev. Mod. Phys. **54**, 235 (1982).

[19] A. Aharony and D. Stauffer, *Introduction to Percolation Theory* (Taylor & Francis, London, 1994).

[20] J. Zarzycki, *Glasses and the Vitreous State* (Cambridge University Press, Cambridge 1991).

[21] W. Kob and H.C. Andersen, Phys. Rev. E **48**, 4364 (1993).

[22] F. Sciortino, P. Gallo, P. Tartaglia, and S.-H. Chen (unpublished).

[23] H.Z. Cummins *et al.*, Physica A **204**, 169 (1994).

[24] J. Jäckle, Rep. Prog. Phys. **49**, 171 (1986).

[25] C.A. Angell, J. Non-Cryst. Solids **73**, 1 (1985).

[26] E. Leutheusser, Phys. Rev. A **29**, 2765 (1984).

[27] U. Bengtzelius, W. Götze, and A. Sjölander, J. Phys. C **17**, 5915 (1984).

[28] T. Tomida and T. Egami, Phys. Rev. B **52**, 3290 (1995).

[29] D. Kivelson *et al.*, Physica A **219**, 27 (1995).

[30] A. Coniglio and H.J. Herrmann, Physica A **225**, 1 (1996); M. Nicodemi, A. Coniglio, and H.J. Herrmann (unpublished).